Article

# Understanding the Role of M/Pt(111) (M = Fe, Co, Ni, Cu) Bimetallic Surfaces for Selective Hydrodeoxygenation of Furfural

Zhifeng Jiang, Weiming Wan, Zhexi Lin, Jimin Xie, and Jingguang G Chen

*ACS Catal.*, **Just Accepted Manuscript** • DOI: 10.1021/acscatal.7b01682 • Publication Date (Web): 24 Jul 2017

# Understanding the Role of M/Pt(111) (M = Fe, Co, Ni, Cu) Bimetallic Surfaces for Selective Hydrodeoxygenation of Furfural

Zhifeng Jiang,[¶a,b] Weiming Wan,[¶b] Zhexi Lin,[b] Jimin Xie,[a] and Jingguang G. Chen[b,c]*

[a]Institute for Energy Research, School of Chemistry and Chemical Engineering, Jiangsu University, Zhenjiang, Jiangsu, 212013, P. R. China

[b]Department of Chemical Engineering, Columbia University, New York, NY, 10027, USA

[c]Chemistry Department, Brookhaven National Laboratory, Upton, NY 11973, USA

Corresponding author: jgchen@columbia.edu (J. G. Chen)

[¶] These authors contributed equally to this work.

**Abstract**

Selectively cleaving the C=O bond of the aldehyde group in furfural is critical for converting this biomass-derived platform chemical to an important biofuel molecule, 2-methylfuran. This work combined density functional theory (DFT) calculations, temperature programmed desorption (TPD) and high-resolution electron energy loss spectroscopy (HREELS) measurements to investigate the hydrodeoxygenation (HDO) activity of furfural on bimetallic surfaces prepared by modifying Pt(111) with 3d transition metals (Cu, Ni, Fe and Co). The stronger binding energy of furfural and higher tilted degree of the furan ring on the Co-terminated bimetallic surface resulted in a higher activity for furfural HDO to produce 2-methylfuran than that on either Pt(111) or Pt-terminated PtCoPt(111). The 3d-terminated bimetallic surfaces with strongly oxophilic 3d metals (Co and Fe) showed higher 2-methylfuran yield than those surfaces modified with weakly oxophilic 3d metals (Cu and Ni). The effect of oxygen on the HDO selectivity was also investigated on oxygen-modified bimetallic surfaces, revealing that the presence of surface oxygen resulted in a decrease in 2-methylfuran yield. The combined theoretical and experimental results presented here should provide useful guidance for designing Pt-based bimetallic HDO catalysts.

**Keywords:** furfural, hydrodeoxygenation, 2-methylfuran, bimetallic surfaces, oxophilicity

## 1. Introduction

Biomass represents sustainable carbon sources for the production of transportation fuels and chemicals.[1] Furfural, one of the most promising platform molecules that is derived from hemicellulose via the hydrolysis and dehydration of xylose, has received significant attention because it offers the advantages of being widely available, renewable, and potentially carbon-neutral.[2] The selective removal of the oxygen atom in the carbonyl group is a major barrier in processing furfural for fuel applications.[3] An ideal hydrodeoxygenation (HDO) catalyst for furfural should selectively cleave the carbonyl C=O bond while keeping the C-O/C-C/C=C bonds of the furan ring intact. The desirable HDO product, 2-methylfuran (2-MF), has shown promise as a fuel additive in a practical road trial (high octane number, RON ~131, energy density and low water solubility).[4]

Bimetallic catalysts often exhibit unique properties that differ from those of their parent metals and offer the opportunity to design catalysts with improved activity and selectivity that exceed those achievable with a monometallic catalyst.[5] For example, Resasco et al.[6] have reported that the aromatic ring hydrogenation of anisole and guaiacol was suppressed when Pt was modified with Sn. Similar result has also been reported by Vohs et al.[7] that alloying Pt with Zn could improve the selectivity for the conversion of furfural to the desired HDO product of 2-MF, while the decarbonylation products, such as furan and CO, were suppressed.

Although traditional precious metal catalysts, such as Pd[8] and Pt[9], exhibit relatively high activity, the undesirable side reactions reduce the HDO selectivity to produce 2-MF. To date, a variety of bimetallic catalysts with different structures were reported for the HDO of furanic molecules.[10] Gorte et al.[10a] studied the HDO of 5-hydroxymethylfurfural over PtCo nanocrystals and found that the $Pt_3Co_2$ (with Pt-rich core and a monolayer Co oxide shell) catalyst showed the highest 2,5-dimethylfuran yield of 98%, which can be attributed to the oxide monolayer that interacts weakly with the furan ring to prevent side reactions. Huang[10b] and co-workers reported that the CuPd alloys showed advantages over the monometallic catalyst in the hydrogenation of furfural to

2-MF and 2-methyltetrahydrofuran (2-MTHF). Yu et al.[10c] prepared a FeNi bimetallic structure and showed that the ML FeNi(111) bimetallic surface had a higher 2-MF yeild toward furfural HDO. In addition, studies concerning the oxidation state of catalysts were widely investigated for the HDO of furanic molecules.[11] The work by Zhang et al.[11a] has shown that compared with $Pd/SiO_2$, the incorporation of $FeO_x$ species into the $Pd/SiO_2$ significantly enhanced the HDO activity of furan compounds, which was attributed to the generation of Pd-Fe alloy and partially reduced $FeO_x$ species in the $Pd\text{-}FeO_x/SiO_2$ system. Vlachos et al.[11b] have studied the reaction of 5-hydroxymethylfurfural over $Ru\text{-}Ru_2O/C$ catalysts and shown that the selective production of 2, 5-dimethylfuran could reach a 72% yield by generating a partially oxidized Ru catalyst. Hronec et al.[11c] reported that the formation of partially oxidized $Cu^+$ in the Pd-Cu/C system favored the selective rearrangement of furfural to cyclopentanone rather than 2-MF.

Considering the uncertainties and/or inconsistencies of the previous work, surface science studies which can control the bimetallic structure (metal-termination) and oxygen modification were performed to investigate their effects on the HDO reaction of furfural. To this end, the primary objective of the current paper is to understand how the modification of the Pt(111) surface by oxophilic metals alters the HDO selectivity of furfural. The results presented here combine density functional theory (DFT) calculations and surface science experiments using temperature programmed desorption (TPD) and high-resolution electron energy loss spectroscopy (HREELS) to study the effect of oxophilic 3d metal/Pt(111) bimetallic surfaces on the adsorption geometry and selective HDO of furfural. The bimetallic surfaces were prepared by modifying Pt(111) with four 3d transition metals with weak (Cu and Ni) or strong (Co and Fe) oxophilicity. Both the subsurface sandwich Pt-3d-Pt(111) structure and the overlayer 3d-Pt-Pt(111) sturcture were investigated. Additionally, the effect of surface oxygen on the HDO of furfural was investigated on oxygen-modified bimetallic surfaces.

## 2. Experimental and computational methods

### 2.1. DFT calculations

All DFT calculations were performed with the Vienna *Ab initio* Simulation Package (VASP) software.[12] The core electrons were represented with the PAW formalism,[13] while the valence region was represented with the PBE exchange-correlation functional.[14,15] Total energies were minimized self-consistently using a convergence threshold of $10^{-6}$ eV. The nuclear degrees of freedom were optimized to a force convergence threshold of 0.05 eV $Å^{-1}$. All slab calculations were performed using a periodic 4 x 4 unit cell of four metal layers, with six equivalent layers of vacuum between slabs. The two bottom layers of the Pt(111) slab were frozen, while the top two layers were allowed to relax to reach the lowest energy configuration. The monolayer 3d-Pt-Pt(111) surfaces were constructed by replacing the top layer of Pt atoms with 3d metal atoms. The subsurface Pt-3d-Pt(111) structures were constructed by replacing the second layer of Pt atoms with 3d metal atoms. The calculations were carried out implenting the spin-polarization. The binding energy of furfural on each surface was calculated by subtracting the energies of the bare slab and free molecule from the total energy of the slab with adsorbed furfural.

### 2.2. Surface science experiments

#### 2.2.1. Preparation of bimetallic surfaces

Single crystal Pt(111) was purchased from Princeton Scientific Corporation. The Pt(111) crystal has a purity of 99.999%, a diameter of 8 mm and a thickness of 1.5 mm. The preparation of 3d/Pt(111) bimetallic structures was performed using identical procedures reported in a previous study.[12] The 3d-Pt-Pt(111) surface structure was prepared by depositing 1 ML of 3d metal on Pt(111) at 300 K. The Pt-3d-Pt(111) subsurface structure was obtained by depositing 1 ML of 3d metal at 600 K, with the 3d metal diffusing beneath the top layer of Pt(111) at this temperature.[12] The 3d metal coverage was estimated using Auger electron spectroscopy (AES) based on the AES peak intensities of Fe(646 eV), Co(777 eV), Ni(718 eV), Cu(922 eV) and Pt(922 eV), as described in a previous study.[12] The Pt(111) surface was cleaned by $Ne^+$ sputtering at 300 K, followed with $O_2$ treatment to remove residual surface carbon, and then annealing at 1050 K. The $O_2$ treatment was repeated until negligible amount of C was detected by AES.

### 2.2.2. TPD measurements

Furfural and 2-MF, purchased from Sigma Aldrich with purity of 99%, were injected into glass cylinders and purified using freeze-pump-throw cycles. All gas samples, hydrogen, neon, and carbon monoxide, were of research purity and used without further purification. The reagents were dosed into the UHV chamber with a stainless steel dosing tube and the purity was verified by mass spectrometry. The TPD experiments were performed in a UHV chamber with a base pressure of $4 \times 10^{-10}$ Torr, equipped with AES, a mass spectrometer, a sputter gun and metal sources, as described previously.[16] The metal source was constructed with a high purity metal wire (Alfa Aesar, 99.99%) wrapped around a tungsten filament and was mounted within a tantalum enclosure. The Pt(111) crystal was placed at the center of the UHV chamber by directly spot-welding to two tantalum posts, allowing resistive heating and cooling with liquid nitrogen.[10c] For the TPD experiments 4 L (1 L = $1x10^{-6}$ Torr.s) furfural and 5 L $H_2$ were first dosed into UHV chamber. The Pt(111) or metal-modified Pt(111) surface was then heated from 110 K to 800 K with a linear rate of 3 K/s and the products desorbing from the surface were detected using a mass spectrometer.

### 2.2.3. HREELS measurements

The HREELS experiments on the Pt(111), PtCoPt(111) and CoPtPt(111) surfaces were performed in a separate UHV chamber with a base pressure of $1\times10^{-10}$ Torr. Each molecule was dosed to as-prepared surfaces at 100 K. During the HREELS measurements, the surfaces were heated to higher temperatures at 3 K/s and cooled down to 100 K before each HREEL spectrum was recorded. The prime beam energy was 6 eV and the angles of the incidence and reflection beam were $60^{o}$ with respect to the surface normal. The count rate of the elastic peak was typically $2 \times 10^{5}$ counts/s and the resolution was 50 $cm^{-1}$ full width at half maximum.

## 3. Results and discussion

### 3.1. Reaction of furfural on Co/Pt(111) surfaces

#### 3.1.1. DFT calculations of furfural on Co/Pt(111) surfaces

DFT calculations of furfural were performed on Pt(111), PtCoPt(111) and CoPtPt(111) surfaces. The top and side views of the optimized configurations of furfural on the three surfaces are shown in Figure 1(A). The numerical assignment of the carbon and oxygen atoms in furfural is shown in Figure 1(B). The correlation between the d-band center and the binding energy of furfural on each surface is presented in Figure 1(C). The binding energy values of furfural are predicted to increase as the surface d-band center moves closer to the Fermi level, in agreement with trends observed for other adsorbates in previous reports.[12, 17] The Co-terminated bimetallic surface shows the highest binding energy of furfural among the three surfaces.

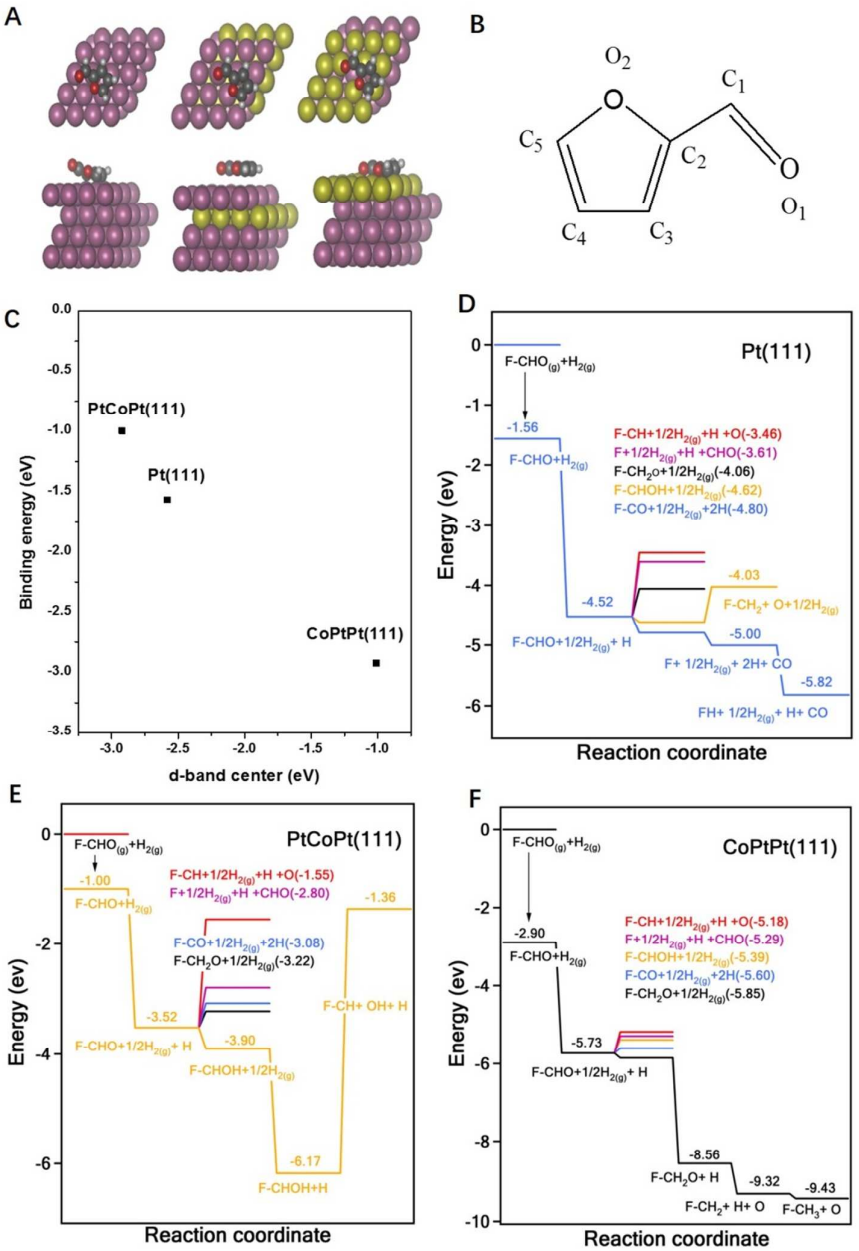

**Figure 1.** (A) Top and side views of DFT-optimized structures of furfural on Pt(111), PtCoPt(111) and CoPtPt(111) surfaces (Pt: fuchsia, Co: kelly, C: gray, O: red, H: white); (B) the assignment of the carbon and oxygen atoms in furfural; (C) the correlation between the d-band center and the binding energy of furfural on each surface; (D-F) DFT calculated binding energies of reaction intermediates of furfural on the Co/Pt(111) surfaces (F = 2-furanyl)

**Table 1** Comparison of bond lengths, bond length ratio and binding energies of furfural adsorbed on the corresponding surfaces

| | Pt(111) | PtCoPt(111) | CoPtPt(111) |
|---|---|---|---|
| $O_1$-M (Å) | 3.444 | 3.093 | 1.903 |
| $O_2$-M (Å) | 2.860 | 3.302 | 2.448 |
| $d(O_2\text{-M})/d(O_1\text{-M})$ | 0.830 | 1.068 | 1.286 |
| Binding energy (eV) | -1.564 | -0.996 | -2.926 |

Table 1 summarizes binding energies (eV) of adsorbed furfural and the tilted degree of the furan ring on the three surfaces. The binding energies of furfural show a trend of CoPtPt(111) > Pt(111) > PtCoPt(111). The bond distances of $O_1$-M and $O_2$-M, and the $d(O_2\text{-M})/d(O_1\text{-M})$ ratio are compared to investigate the extent of the furan ring tilting away from the surface. The distances of $O_1$-M and $O_2$-M on Co-terminated CoPtPt(111) are smaller than those on Pt(111) and PtCoPt(111), indicating that furfural has stronger interaction with the Co-terminated bimetallic surface than the other two, consistent with the higher furfural binding energy on CoPtPt(111). The $d(O_2\text{-M})/d(O_1\text{-M})$ ratio of furfural shows a trend of CoPtPt(111) > PtCoPt(111) > Pt(111), suggesting that the addition of 1 ML Co on Pt(111) makes the furan ring of furfural tilted further away from the surface.

In order to predict the reaction pathways of furfural on Co/Pt(111) surfaces, the reaction energies of five possible reaction intermediates were calculated. As shown in Figure 1D-F**,** possible intermediates from furfural include F-CHOH (orange line, F = 2-furanyl) or F-$CH_2O$ (black line) through hydrogenation, F-CH (red line) by C=O bond cleavage, furanyl (purple line) through C-C bond scisson and FCO (blue line) by dehydrogenation. The Bronsted–Evans–Polanyi principle suggests that a more negative reaction energy should in general lead to a lower activation barrier.[18] On the Pt(111) surface (Figure 1D), the dehydrogenation of furfural is perferred as the first step and all the following steps in the blue curve are exothermic, suggesting that F-CO would break the C-C bond to form CO and furanyl, which would be further hydrogenated to form furan. Figure 1E shows that on PtCoPt(111) furfural can be converted to F-CHOH in the first step through hydrogenation.

However, it is unfavorable to break the C-O bond of F-CHOH to form F-CH, suggesting that the PtCoPt(111) surface should have a low HDO activity. Since furfural has a low binding energy on PtCoPt(111), the molecular desorption of furfural would likely occur before undergoing subsequent surface reactions. On the CoPtPt(111) surface (Figure 1F), furfural prefers to be hydrogenated to form F-$CH_2O$ in the first step. It is also favorable to break the C-O bond of F-$CH_2O$ to form F-$CH_2$ and surface oxygen, with F-$CH_2$ being further hydrogenated to form 2-MF.

In summary, DFT calculations provide two parameters to predict the surface activity: the binding energy of furfural and the tilted degree of the furan ring. The surface with high furfural binding energy and a tilted furan ring, CoPtPt(111), prefers to produce 2-MF. The surface with high furfural binding energy and a flat furan ring, Pt(111), prefers to produce furan. Finally, the surface with low binding energy, PtCoPt(111), should have a low activity for furfural conversion.

### 3.1.2. TPD experiments of furfural on Co/Pt(111) surfaces

TPD experiments were performed to investigate the products from Pt(111), PtCoPt(111) and CoPtPt(111) surfaces after exposure to 5 L $H_2$, corresponding to half of the saturated H coverage, and 4 L furfural, corresponding to a saturation of chemisorbed furfural. Some of the possible reaction pathways of furfural are listed as follows:

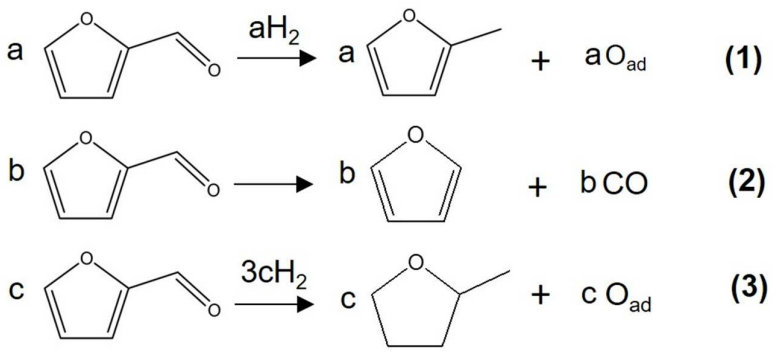


Reaction (1) represents the desired HDO reaction as it produces 2-MF, reaction (2) is the undesired decarbonylation pathway involving the $C_1$-$C_2$ bond scission to produce furan and CO, and reaction (3) includes both HDO and the hydrogenation of the furan ring to produce 2-MTHF and $O_{ad}$. The stoichiometric coefficients in the above equations, a, b and c, represent the amount of chemisorbed furfural (molecule per metal atom) to produce 2-MF, furan and 2-MTHF, respectively. The yields

of the above-mentioned gas-phase products are estimated from the TPD peak areas of the cracking patterns of 2-MF (m/e = 82), furan (m/e = 68) and 2-MTHF (m/e = 71), as shown in Figure 2.

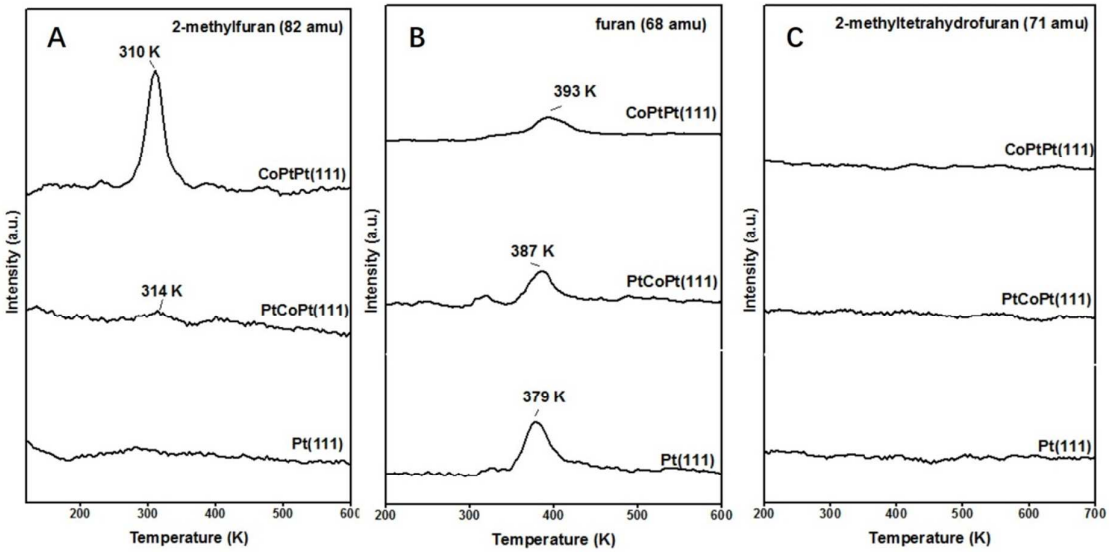


**Figure 2.** TPD spectra of (A) 2-MF (m/e = 82), (B) furan (m/e = 68) and (C) 2-MTHF (m/e = 71) with an exposure of 4 L furfural on hydrogen pre-dosed Pt(111), PtCoPt(111) and CoPtPt(111) surfaces.

The molecular desorption of furfural from the as-prepared surfaces occurs at about 200 K (spectra not shown). As can be observed from Figure 2A, the desorption peak of 2-MF is observed at 310 K from CoPtPt(111), while only trace amount of 2-MF is observed from PtCoPt(111) and 2-MF is not detected from the Pt(111)[4d] surface. Figure 2B shows the production of furan from the decarbonylation pathway. The Pt(111) surface produces the largest amount of furan among the three surfaces, which is consistent with the conclusion from the Kyriakou group.[4d] Figure 2C indicates that 2-MTHF is not produced from the three surfaces under UHV conditions. In addition to the furan-ring containing products, ethylene was also detected as a reaction product as shown in Figure S1 and Table S1 in the Supporting Information. To quantify the amount of furfural undergoing each of the above-mentioned reaction pathways, the yields of 2-MF, furan and 2-MTHF were calculated from an experimentally determined sensitivity factor relative to CO by comparing the mass spectrometer sensitivity factors at equal concentrations of 2-MF, furan,2-MTHF and CO. According to the reported literature,[19a] the saturation coverage of CO on Pt(111) is 0.68 ML ($\theta_{CO}^{sat}$ = 0.68) and this value is used for the quantification. Detailed procedures for quantifying the TPD products were

described in a previous work.[19b] Table 2 summarizes the activity and selectivity of furfural on Pt(111), PtCoPt(111) and CoPtPt(111) surfaces.

The 2-MF yield follows the trend of CoPtPt(111) > PtCoPt(111) ≈ Pt(111) and the furan yield follows the trend of Pt(111) > PtCoPt(111) > CoPtPt(111). The TPD results are consistent with the DFT predictions (Figure 1) that CoPtPt(111) is active toward 2-MF formation, Pt(111) is active to form furan, and PtCoPt(111) has the lowest activity for furfural decomposition.

**Table 2** Quantification of furfural on hydrogen pre-dosed Co/Pt(111) surfaces from TPD measurements

| | Activity (monolayer per metal atom) | | | | Selectivity of furan-ring containing products (%) | |
|---|---|---|---|---|---|---|
| | 2-MF | Furan | 2-MTHF | Total | 2-MF | Furan |
| Pt(111) | 0 | 0.036 | 0 | 0.036 | 0 | 100 |
| PtCoPt(111) | 0.001 | 0.018 | 0 | 0.019 | 5.3 | 94.7 |
| CoPtPt(111) | 0.012 | 0.008 | 0 | 0.020 | 60.0 | 40.0 |

### 3.1.3. HREELS measurements of furfural on Co/Pt(111) surfaces

The HREELS experiments were performed to determine the adsorption configuration of furfural and to identify surface reaction intermediates on Pt(111), PtCoPt(111) and CoPtPt(111). The vibrational features of furfural observed at 100 K are summarized in Table 3, along with Raman frequencies of liquid furfural. Figure 3 shows the HREELS spectra of 4 L furfural on hydrogen pre-dosed Pt(111), PtCoPt(111) and CoPtPt(111) surfaces at 100 K and the vibrational frequencies were generally similar with those of the Raman spectrum of liquid furfural, suggesting that furfural adsorbed molecularly on the three surfaces at 100 K. After the surfaces were heated to 200 K, the intensities of all vibrational modes decreased. The relative intensiy of the $\nu(CH)_{ring}$ at 3080 $cm^{-1}$ decreased compared to that of the $\nu(CH)_{aliphatic}$ at 2838 $cm^{-1}$, indicative of the interaction between the skeletal furan structure and metal surfaces. Meanwhile, the intensity of the $\nu$(C=O) mode at 1643 $cm^{-1}$ decreased and shifted to a lower frequency, resulting from the interaction between the carbonyl group and the metal surfaces to form the $\eta^2$(C,O)-furfural intermediate, as predicted from the DFT results.

A comparison of the HREELS spectra at 200 K provides information about the adsorption configuration of furfural on the three surfaces. Vibrational peaks at 1440 $cm^{-1}$ and 1643 $cm^{-1}$ represent ν(C=C) in the furan ring and ν(C=O) in the carbonyl group, respectively. The ratio of these two peaks, I(1440)/I(1643) (defined as $\alpha$) could be used to provide a qualitative indicator regarding the relative orientation of the furan ring in furfural with respect to the carbonyl group. As compared in Table 4, $\alpha$ on CoPtPt(111) showed the highest value, indicating that the furan ring in adsorbed furfural is tilted to the largest extent on CoPtPt(111) compared with that of Pt(111) and PtCoPt(111), in agreement with the DFT prediction.

**Table 3.** Vibrational assignment of furfural

| Mode | Frequency($cm^{-1}$) | | | |
|---|---|---|---|---|
| | Raman[a] | Pt(111)[b] | PtCoPt (111)[c] | CoPtPt(111)[d] |
| τ (ring) | -- | 602 | 602 | 605 |
| ω (CH) | -- | 765 | 765 | 760 |
| δ (ring) | -- | -- | -- | -- |
| ν (CO) | 930 | -- | -- | -- |
| χ (CH) | 950 | -- | -- | -- |
| ν (CO) | 1025 | 1023 | 1016 | 1018 |
| $\delta_b$ (O-C-H) | 1157 | 1131 | 1141 | 1133 |
| ρ (CH) | -- | 1223 | 1202 | 1216 |
| $\delta_b$ (O-C-H) | 1370 | -- | -- | -- |
| ν (CC) | 1395 | -- | -- | -- |
| ν (C=C) | 1466, 1555, 1570 | 1445 | 1440 | 1437 |
| ν (C=O) | 1684 | 1650 | 1654 | 1643 |
| ν (CH) | -- | 2832 | 2827 | 2837 |
| ν (CH) | 3153 | 3087 | 3080 | 3090 |

τ - torsion, ω - wagging, δ - deformation, ν - symmetric stretching, χ - scissoring, $\delta_b$ - bending, ρ - rocking

[a] Ref. [10c]

[b] 4 L furfural on Pt(111) at 100 K

[c] 4 L furfural on PtCoPt(111) at 100 K

[d] 4 L furfural on CoPtPt(111) at 100 K

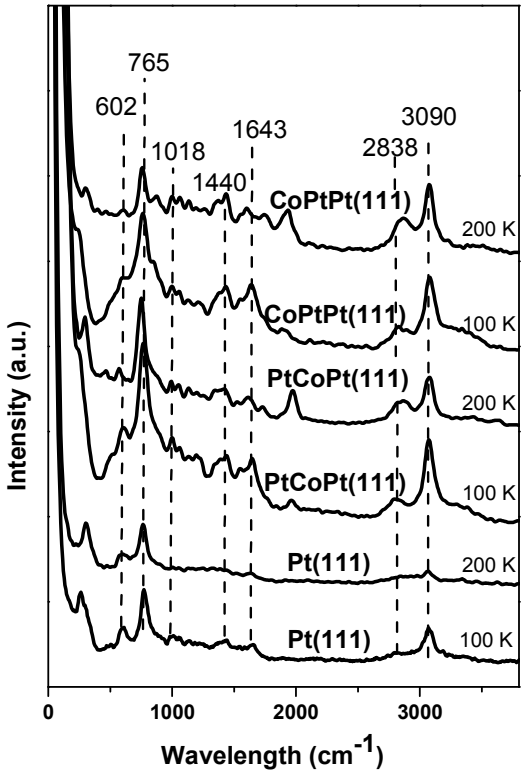


**Figure 3.** HREELS of 4 L furfural on $H_2$ pre-dosed Pt(111), PtCoPt(111) and CoPtPt(111) surfaces at 100 Kand 200 K.

**Table 4.** Intensity ratio of I(1440)/I(1643) in HREEL spectra of furfural adsorption on $H_2$ pre-dosed Pt(111), PtCoPt(111) and CoPtPt(111) surfaces

| Surface | Temperature (K) | I(1440)/I(1643) |
|---|---|---|
| Pt(111) | 200 | 0.9 |
| PtCoPt(111) | 200 | 1.2 |
| CoPtPt(111) | 200 | 2.8 |

The on- and off-specular HREELS measurements were further carried out to determine the different adsorption configurations of furfural on the three surfaces. Based on the surface dipole selection rule, virbrational modes with component of dipole moment perpendicular to the surface would have a strong signal in the on-specular spectra. Thus, the virbrational modes that are more tilted away from the surface should show higher intensity in the on-specular spectra and relatively low intensity in the off-specular spectra. The on- and off-specular HREELS spectra of 4 L furfural at 200 K on hydrogen pre-dosed Pt(111), PtCoPt(111) and CoPtPt(111) surfaces are presented in Figure 4. The vibrational peaks at 765 $cm^{-1}$ and 1643 $cm^{-1}$ represent the ω(C-H) mode of the furan ring and the ν(C=O) mode of the carbonyl group, respectively. The ratio of these two modes, (I(765)/I(1643)), is

defined as $\beta$ and this value is used to compare the relative tilted degree of the furan ring and carbonyl group. As shown in Table 5, the $\beta$ values of the on-specular spectra for Pt(111), PtCoPt(111) and CoPtPt(111) follow a trend of 10.7 > 8.4 > 2.6, suggesting that the furan ring in furfural adsorbed more parallel to the Pt(111) and PtCoPt(111) surfaces than to CoPtPt(111). In the off-specular spectra, the $\beta$ values on Pt(111) and PtCoPt(111) surfaces decreased from 10.7 to 1.8 and 8.4 to 5.2. In contrast, on the CoPtPt(111) surface, $\beta$ remained similar in the on- and off-specular measurements from 2.6 to 2.9. The differences in the $\beta$ values further suggest that the furan ring in furfural is tilted in a larger angle than the carbonyl group on the CoPtPt(111) surface.

The HREELS analysis provides evidence to support the DFT prediction that the furan ring of furfural is more tilted on CoPtPt(111) than on Pt(111). The titlted configuration of furfural on the CoPtPt(111) surface allows a stronger interaction with the carbonyl group than with the furan ring, leading to the selective HDO through the carbonyl group to produce 2-MF, consistent with the DFT predictions and the TPD experimental results.

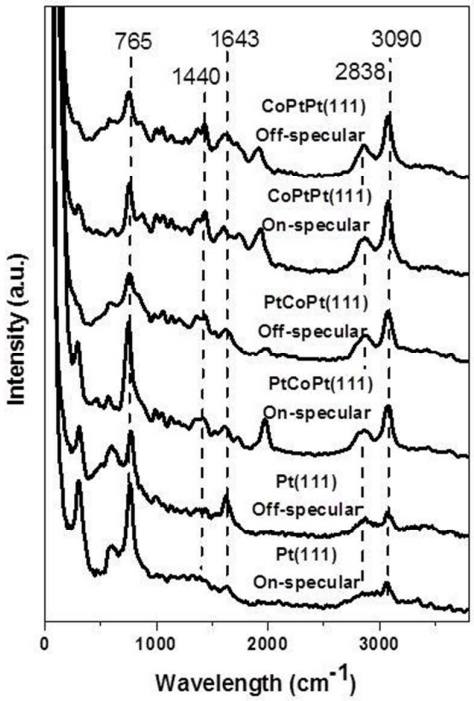


**Figure 4.** On and off-specular HREELS of 4 L furfural on $H_2$ pre-dosed Pt(111), PtCoPt(111) and CoPtPt(111) surfaces at 200 K.

**Table 5.** Intensity ratio of I(765)/I(1643) in HREELS spectra of furfural adsorption on $H_2$ pre-dosed Pt(111), PtCoPt(111) and CoPtPt(111) surfaces

| Surface | Type | I(765)/I(1643) |
|---|---|---|
| Pt(111) | On-specular | 10.7 |
| | Off-specular | 1.8 |
| PtCoPt(111) | On-specular | 8.4 |
| | Off-specular | 5.2 |
| CoPtPt(111) | On-specular | 2.6 |
| | Off-specular | 2.9 |

### 3.2. Trend in furfural reaction on M/Pt(111) (M = Cu, Ni, Fe and Co) surfaces

#### 3.2.1. DFT calculations of furfural and oxygen on M/Pt(111) surfaces

In the previous section, two parameters, furfural binding energy and tilted degree of the furan ring, were used to explain the HDO activity over Co/Pt(111) surfaces. This section will attempt to use these two parameters to predict the performance of other 3d/Pt(111) surfaces. Since the ML CoPtPt(111) structure shows better HDO activity and selectivity than PtCoPt(111), only the M-terminated bimetallic surfaces (M = Cu, Ni, Fe and Co) will be compared here. As summarized in Table 6, the NiPtPt(111), FePtPt(111) and CoPtPt(111) surfaces show similar binding energies of furfural, which are much larger than that of CuPtPt(111). This could be attributed to the different absorbed configuration of furfural on these four surfaces. Furfural absorbs on NiPtPt(111), FePtPt(111) and CoPtPt(111) in the $\eta^2$(C-O) configuration in which both the C and O of carbonyl group are bonded to the surface, whereas the adsorption on CuPtPt(111) adopts a top $\eta^1$(O)-aldehyde[20] binding mode. The ratio of $d(O_2\text{-M})/d(O_1\text{-M})$ follows the order of CuPtPt(111) > CoPtPt(111) > FePtPt(111) > NiPtPt(111) (Table 6). Although the furan ring in furfural is tilted in the largest angle to CuPtPt(111) as compared to the other three surfaces, the HDO activity of CuPtPt(111) may not be the highest because of the weak binding energy of furfural on the surface.

In addition, as indicated by the oxygen binding energies (Table 6), CoPtPt(111) and FePtPt(111) surfaces are stronger oxophilic surfaces than NiPtPt(111) and CuPtPt(111). Correspondingly, the CoPtPt(111) and FePtPt(111) surfaces have the smallest $d(O_1\text{-M})$ value, suggesting that these two oxophilic surfaces have stronger interaction with the carbonyl group of furfural, which should facilitate the cleavage of the C=O bond and lead to HDO activity. In terms of the degree of the tilted

ring, the $d(O_2\text{-M})/d(O_1\text{-M})$ value is slightly lower on FePtPt(111) than the CoPtPt(111) surface, suggesting that the furan ring is more tilted on CoPtPt(111).

**Table 6** Comparison of bond lengths, bond length ratio and binding energies of oxygen and furfural adsorbed on the corresponding surfaces.

| | CuPtPt(111) | NiPtPt(111) | FePtPt(111) | CoPtPt(111) |
|---|---|---|---|---|
| OBE* (eV) | -6.30 | -7.62 | -8.59 | -7.85 |
| $O_1$-M (Å) | 2.049 | 1.930 | 1.901 | 1.903 |
| $O_2$-M (Å) | 3.077 | 2.105 | 2.176 | 2.448 |
| $d(O_2\text{-M})/d(O_1\text{-M})$ | 1.502 | 1.091 | 1.144 | 1.286 |
| Binding energy (eV) | -1.665 | -3.256 | -3.496 | -2.926 |

*OBE = Oxygen binding energy

### 3.2.2 TPD experiments of furfural on M/Pt(111) bimetallic surfaces

As shown in Figure 5, TPD experiments on the four bimetallic surfaces were further carried out to verify the DFT prediction. The adsorbed molecular furfural desorbed at about 200 K from the four bimetallic surfaces (spectra not shown). The CoPtPt(111), FePtPt(111) and NiPtPt(111) surfaces show 2-MF activity while CuPtPt(111) does not show HDO activity (Figure 5A), which could be attributed to the weak furfural binding energy. Furan desorption occurs between 378 and 393 K from all the bimetallic surfaces (Figure 5B). No 2-MTHF desorption peak was observed from all the surfaces (Figure 5C). Among three surfaces with HDO activity, the 2-MF yield shows a trend of CoPtPt(111) > FePtPt(111) > NiPtPt(111) (Table 7), which is consistent with the trend of the tilted degree predicted by DFT calculations. In contrast, the furan yield shows the opposite trend of NiPtPt(111) > FePtPt(111) > CoPtPt(111) (Table 7), which is consistent with the argument that a less tilted furan ring would facilitate the $C_1$-$C_2$ bond cleavage to produce furan. Likewise, the reforming product of ethylene is also generated from the CoPtPt(111), FePtPt(111) and NiPtPt(111) surfaces. From the DFT calculations and TPD results, it is evident that high furfural binding energy is necessary to achieve HDO activity and the tilted degree of the furan ring affects the selectivity. Adsorbed furfural with a more tilted furan ring prefers to form 2-MF, while furfural with a less tilted furan ring leads to decarbonylation to form furan and CO. Therefore, high furfural binding energy and tilted furan ring are both necessary for selective HDO. In addition, both CoPtPt(111) and FePtPt(111) show high yield of 2-MF and they are also strongly oxophilic surfaces. Though the

oxygen binding energy alone is not sufficient to predict the HDO selectivity, in general oxophilic surfaces should show higher HDO activity since it binds more strongly with oxygen of the carbonyl group, facilitating the cleavage of the C=O bond.

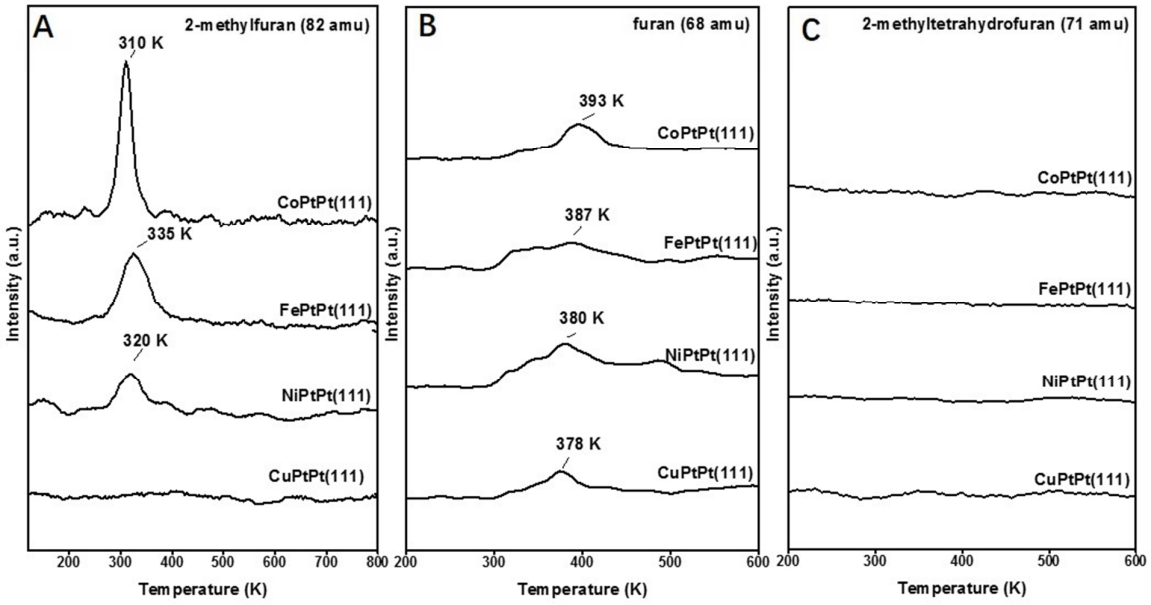


**Figure 5.** TPD spectra of (A) 2-MF (m/e = 82), (B) furan (m/e = 68) (C) 2-MTHF (m/e = 71) with an exposure of 4 L furfural on hydrogen pre-dosed CuPtPt(111), NiPtPt(111), FePtPt(111) and CoPtPt(111) surfaces.

**Table 7** Quantification of furfural on hydrogen pre-dosed M-Pt-Pt(111) surfaces from TPD measurements

| | Activity (monolayer per metal atom) | | | | Selectivity of furan-ring containing product (%) | |
|---|---|---|---|---|---|---|
| | 2-MF | Furan | 2-MTHF | Total | 2-MF | Furan |
| CuPtPt(111) | 0 | 0.008 | 0 | 0.008 | 0 | 100 |
| NiPtPt(111) | 0.004 | 0.024 | 0 | 0.028 | 14.3 | 85.7 |
| FePtPt(111) | 0.010 | 0.015 | 0 | 0.025 | 40.0 | 60.0 |
| CoPtPt(111) | 0.012 | 0.008 | 0 | 0.020 | 60.0 | 40.0 |

### 3.2.3. Effect of oxygen-modification on M/Pt(111) bimetallic surfaces

In many reactor studies, HDO catalysts were reported to be partially oxidized during the HDO reactions. For example, Vlachos et al.[21] reported $Ru/RuO_x/C$ to be active for furfural HDO. Zhang et al.[11a] reported $Pd/FeO_x$ as an active catalyst for HDO of furan compounds. Gorte et al.[10a] reported that the formation of a $CoO_x$ overlayer on Pt was responsible for the high activity and selectivity toward furfural HDO. It remains unclear whether the oxophilicity of the metal or the presence of

surface oxygen contributes to the HDO activity. Thus, furfural TPD experiments were performed on clean and oxygen-modified M-Pt-Pt(111) (M = Cu, Ni, Fe and Co) surfaces to determine the effect of surface oxygen on furfural HDO. As shown in Figure 6(A), the 2-MF product was not detected from CuPtPt(111), 0.1O/CuPtPt(111) and 0.25O/CuPtPt(111) (0.1 and 0.25 represent the atomic ratios of O/Pt), suggesting that partially oxidizing Cu on CuPtPt(111) surface did not have obvious influence on the 2-MF yield. As shown in Figure 6(B-D) for NiPtPt(111), FePtPt(111), CoPtPt(111), the 2-MF desorption peak area decreased after the surfaces were modified by oxygen. As the oxygen amount increased, the desorption peak areas of 2-MF decreased obviously on all three surfaces, indicating that the presence of oxygen on these bimetallic surface is not in favor of producing 2-MF. Similarly, the yields of other generated products such as furan and ethylene also decreased after the surfaces were modified by oxygen (Figure S2). Based on the TPD results, two general conclusions can be reached: (1) the production of 2-MF is attributed to the overlayer metal surfaces rather than metal oxide-Pt-Pt(111) surfaces; (2) the addition of oxygen likely blocks the activate sites of the bimetallic surfaces, resulting in a significant decrease in the yield of 2-MF.

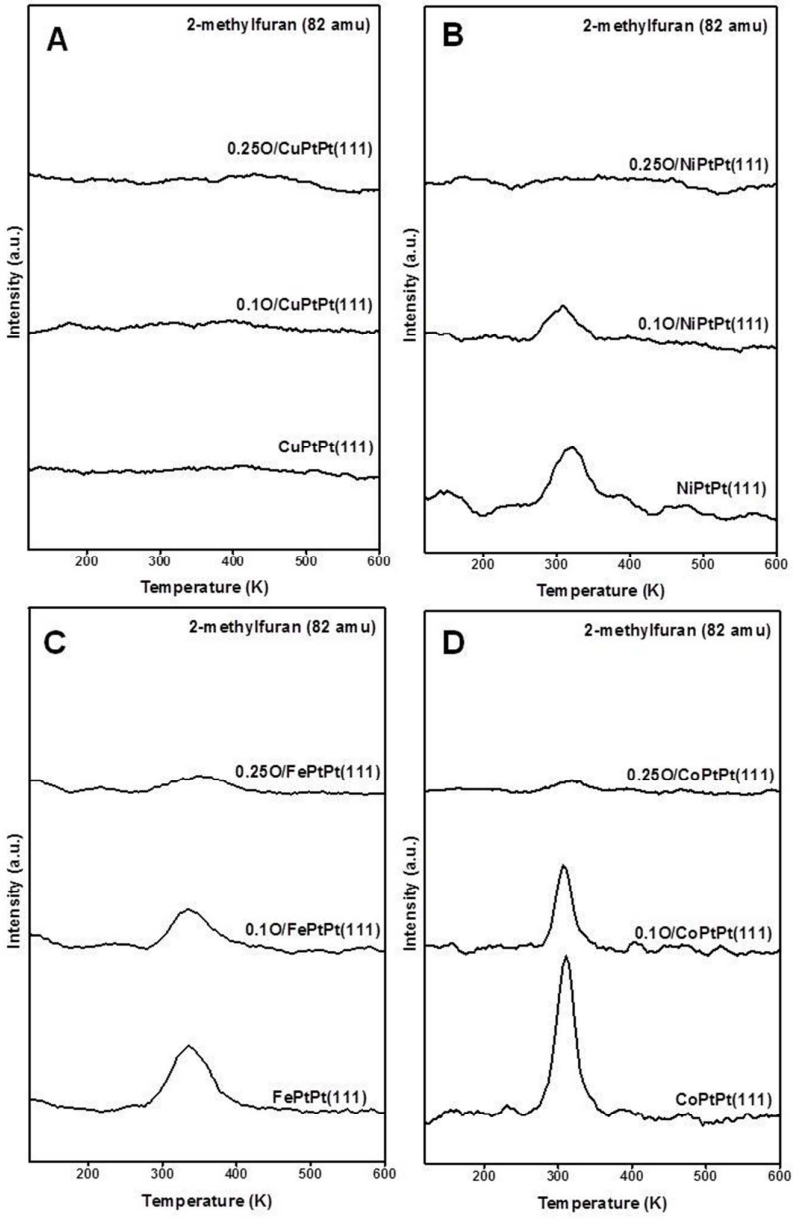


**Figure 6.** TPD spectra of 2-MF (m/e = 82) with an exposure of 4 L furfural on hydrogen pre-dosed oxygen-modified M-Pt-Pt(111) surfaces (M = Cu, Ni, Fe and Co).

## 4. Conclusions

In summary, combined DFT calculations and surface science experiments were performed to study the HDO reaction on 3d/Pt(111) bimetallic surfaces using furfural as a probe molecule for biomass-derived oxygenates. The main conclusions are as follows:

(1) For the reaction of furfural on Co/Pt(111) surfaces, the Co-terminated CoPtPt(111) surface shows higher HDO activity for furfural to produce 2-MF than the Pt-terminated PtCoPt(111) surface. The addition of ML Co atoms onto Pt(111) increases the furfural binding energy and

leads to the furan ring in furfural tilted away from the surface, as predicted by DFT calculations and confirmed by the on- and off- specular HREELS results. Reaction network DFT calculation also suggests that the addition of Co atoms can alter the reaction pathway of furfural to form 2-MF.

(2) For 3d-terminated bimetallic surfaces, the 2-MF yield follows the order of CoPtPt(111) > FePtPt(111) > NiPtPt(111) > CuPtPt(111). The high furfural binding energy is necessary for a surface to show HDO activity and the tilted furan ring can further improve the selectivity. CoPtPt(111) has similar furfural binding energy with FePtPt(111) and NiPtPt(111) while showing the largest tilted degree of furan ring, which facilitates the selective HDO of furfural to produce 2-MF. In contrast, 2-MF is not observed from CuPtPt(111), which can be attributed to the weak interaction with furfural.

(3) Based on the comparison of the HDO activity before and after modifying bimetallic surfaces with oxygen, the production of 2-MF is related to the bimetallic surfaces rather than metal oxide-Pt-Pt(111) surfaces. The addition of surface significantly decreases the yield of 2-MF.

**Acknowledgement**

This article was based on work supported as part of the Catalysis Center for Energy Innovation (CCEI), an Energy Frontier Research Center (EFRC) funded by the U.S. Department of Energy, Office of Basic Energy Sciences under Award Number DE-SC0001004. The DFT calculations were performed using computational resources at the Center for Functional Nanomaterials, a user facility at BNL, supported by US Department of Energy under Contract No. DE-AC02-05CH11231.

**Supporting Information**

Supporting Information Available: additional TPD results for ethylene and furan desorption on the M/Pt(111) and oxygen modified M/Pt(111) surfaces.

This material is available free of charge via the Internet at http://pubs.acs.org.

## Reference

(1) (a) Mariscal, R.; Maireles-Torres, P.; Ojeda, M.; Sádaba, I.; Granados, M. L. *Energ. Environ. Sci.* **2016**, *9*, 1144-1189. (b) Huber, G. W.; Iborra, S.; Corma, A. *Chem. Rev.* **2006**, *106*, 4044-4098. (c) Corma, A.; Iborra, S.; Velty, A. *Chem. Rev.* **2007**, *107*, 2411-2502.

(2) (a) Xiong, K.; Yu, W.; Vlachos, D. G.; Chen, J. G. *ChemCatChem* **2015**, *7*, 1402-1421. (b) Xiong, K.; Lee, W. S.; Bhan, A.; Chen, J. G. *ChemSusChem* **2014**, *7*, 2146-2149.

(3) (a) Wang, H.; Male, J.; Wang, Y. *ACS Catal.* **2013**, *3*, 1047-1070. (b) Vlachos, D. G.; Chen, J. G.; Gorte, R. J.; Huber, G. W.; Tsapatsis, M. *Catal. Lett.* **2010**, *140*, 77-84.

(4) (a) Lee, W.-S.; Wang, Z.; Zheng, W.; Vlachos, D. G.; Bhan, A. *Catal. Sci. Technol.* **2014**, *4*, 2340-2352. (b) Lange, J. P.; van der Heide, E.; van Buijtenen, J.; Price, R. *ChemSusChem* **2012**, *5*, 150-166. (c) Román-Leshkov, Y.; Barrett, C. J.; Liu, Z. Y.; Dumesic, J. A. *Nature* **2007**, *447*, 982-985. (d) M. J. Taylor, L. Jiang, J. Reichert, A. C. Papageorgiou, S. K. Beaumont, K. Wilson, A. F. Lee, J. V Barth, G. Kyriakou. *J. Phys. Chem. C* **2017**, *121*, 8490-8497. (e) J. Luo, M. Monai, H. Yun, L. Arroyo-Ramírez, C. Wang, C. B. Murray, P. Fornasiero, R. J. Gorte. *Catal. Lett.* **2016**, *146*, 711-717.

(5) (a) Pallassana, V.; Neurock, M.; Hansen, L. B.; Nørskov, J. K. *J. Chem. Phys.* **2000**, *112*, 5435-5439. (b) Greeley, J.; Mavrikakis, M. *Nat. Mater.* **2004**, *3*, 810-815. (c) Kitchin, J. R.; Nørskov, J. K.; Barteau, M. A.; Chen, J. *Phys. Rev. Lett.* **2004**, *93*, 156801-156804.

(6) González-Borja, M. Á.; Resasco, D. E. *Energy Fuels* **2011**, *25*, 4155-4162.

(7) Shi, D.; Vohs, J. M. *ACS Catal.***2015**, *5*, 2177-2183.

(8) (a) Sitthisa, S.; Resasco, D. E. *Catal. Lett.* **2011**, *141*, 784-791. (b) Zhao, C.; Kou, Y.; Lemonidou, A. A.; Li, X.; Lercher, J. A. *Angew. Chem. Int. Ed.* **2009**, *121*, 4047-4050. (c) Kim, S. M.; Lee, M. E.; Choi, J.-W.; Suh, D. J.; Suh, Y.-W. *Catal. Commun.* **2011**, *16*, 108-113.

(9) (a) Gutierrez, A.; Kaila, R.; Honkela, M.; Slioor, R.; Krause, A. *Catal. Today* **2009**, *147*, 239-246. (b) Runnebaum, R. C.; Nimmanwudipong, T.; Limbo, R. R.; Block, D. E.; Gates, B. C. *Catal. Lett.* **2012**, *142*, 7-15.

(10) (a) Luo, J.; Yun, H.; Mironenko, A.; Goulas, K.; Lee, J.; Monai, M.; Wang, C.; Vorotnikov, V.; Murray, C.; Vlachos, D.; Fornasiero, P.; Gorte. R. *ACS Catal.* **2016**, *6*, 4095-4104. (b) Chang, X.; Liu, A.; Cai, B; Luo, J.; Pan, H.; Huang, Y. *ChemSusChem* **2016**, *9*, 3330-3337. (c) Yu, W.; Xiong, K.; Ji, N.; Porosoff, M. D.; Chen, J. G. *J. Catal.* **2014**, *317*, 253-262.

(11) (a) Yang, J.; Li, S.; Zhang, L.; Liu, X.; Wang, J.; Pan, X.; Li, N.; Wang, A.; Cong, Y.; Wang, X.; Zhang, T. *Appl. Catal. B: Environ.* **2017**, *201*, 266-277. (b) Jae, J.; Zheng, W.; Karim, A.; Guo, W.; Lobo, R.; Vlachos, D. *ChemCatChem* **2014**, *6*, 848-856. (c) Hroneca, M.; Fulajtárováa, K.; Vávrab, I.; Sotáka,T.; Dobročkab, E.; Mičušíkc, M. *Appl. Catal. B: Environ.* **2016**, *181*, 210-219.

(12) Humbert, M. P.; Chen, J. G. *J. Catal.* **2008**, *257*, 297-306.

(13) (a) Kresse, G.; Furthmuller, J. *Phys. Rev. B* **1996**, *54*, 11169-11186. (b) Kresse, G.; Hafner, J. *Phys. Rev. B* **1993**, *47*, 558-561. (c) Kresse, G.; Hafner, J. *Phys. Rev. B* **1994**, *49*, 14251-14269.

(14) (a) Blöchl, P. E. *Phys. Rev. B* **1994**, *50*, 17953-17979. (b) Spear, K. E.; Frenklach, M. *Pure Appl. Chem.* **1994**, *66*, 1773-1782.

(15) Perdew, J. P.; Burke, K.; Ernzerhof, M. *Phys. Rev. Lett.* **1996**, *77*, 3865-3868.

(16) Salciccioli, M.; Yu, W.; Barteau, M. A.; Chen, J. G.; Vlachos, D. G. *J. Am. Chem. Soc.* **2011**, *133*, 7996-8004.

(17) Yu, W.; Barteau, M. A.; Chen, J. G. *J. Am. Chem. Soc.* **2011**, *133*, 20528-20535.

(18) Evans, M. G.; Polanyi, M. *Trans. Faraday Soc.* **1936**, *32*, 1333-1360.

(19) (a) G. Ertl, M. Neumann, and K. M. Streit, *Surf. Sci.* **1977**, *64*, 393-410. (b) Myint, M.; Yan, Y.; Chen, J. G. *J. Phys. Chem. C* **2014**, *118*, 11340-11349.

(20) Sitthisa, S.; Sooknoi, T.; Ma, Y.; Balbuena, P. B.; Resasco, D. E. *J. Catal.* **2011**, *277*, 1-13.

(21) Gilkey, M.; Panagiotopoulou, P.; Mironenko, A.; Jennes, G.; Vlachos, D.; Xu, B. *ACS Catal.* **2015**, *5*, 3988-3994.

**TOC**